

Second Stokes component generation in the SRS of chirped laser pulses

A.V. Konyashchenko, L.L. Losev, S.Yu. Tenyakov

Abstract. An experimental investigation was made of optical schemes for the generation of the second Stokes component in the SRS of broadband chirped laser pulses in high-pressure gases. Measurements were made of the energy conversion efficiency and the spatial characteristics of the light beam of the second Stokes component for one- and two-fold focusing of the pump radiation into the gas-filled cell as well as in schemes involving a quartz capillary and two gas-filled cells. The highest energy efficiency of conversion to the second Stokes component was attained in the case of cascade generation in the optical scheme with two pressurised-gas cells. In the SRS in hydrogen in this scheme, the Ti:sapphire laser radiation with a wavelength of 0.79 μm was converted to the 2.3- μm second Stokes component with an efficiency of 8.5%.

Keywords: femtosecond pulses, Stimulated Raman scattering.

1. Introduction

At the present time, active research is underway to develop high-power femtosecond laser systems for the near- and medium-IR ranges. Femtosecond lasers with a radiation wavelength $\lambda = 1.5 - 3 \mu\text{m}$ are required for executing experiments in the generation of high-order harmonic [1, 2] and attosecond light pulses [3], in laser chemistry [4, 5], etc. One way to develop such femtosecond laser systems consists in the generation of Stokes pulses in the SRS of the radiation of widely employed lasers – Ti:sapphire lasers ($\lambda \sim 0.8 \mu\text{m}$), ytterbium lasers ($\sim 1 \mu\text{m}$), chromium forsterite lasers ($\sim 1.2 \mu\text{m}$).

The lowering of the carrier frequency of a laser pulse shorter than 100 fs by way of SRS is effected mainly according to the following scheme. First, the pulse is chirped

in frequency by passing it through a dispersion element. In this case, the pulse duration is substantially increased, up to 0.1–1 ns. This is required to lower the radiation intensity in the conversion region and thereby suppress the competing nonlinear effects (phase self-modulation, self-focusing). In the course of SRS of a chirped laser pulse, the chirp of the Stokes pulse reproduces the chirp of the pump pulse. At the final stage of frequency conversion, the Stokes pulse is compressed in time. This scheme was proposed and implemented by Jordan et al. [6]. Its disadvantages are a several-fold lengthening of the Stokes pulse in comparison with the duration of the initial laser pulse and a low reproducibility of the Stokes pulse shape. Subsequent improvement of the optical scheme enabled eliminating these disadvantages and effecting high-efficiency conversion to the first Stokes component with a pulse duration close to that of the pump pulse in gaseous [7, 8] and crystal [9] active media.

The generation of even longer-wavelength radiation in the SRS and hence the broadening of the application area of the laser system may be realised by way of generation of the second Stokes component. For instance, with the use of a Ti:sapphire laser and hydrogen as the Raman-active medium, the wavelength of the second Stokes component will be equal to $\sim 2.5 \mu\text{m}$.

The key parameters in the development of a nonlinear SRS-based femtosecond converter are the conversion efficiency and the spatial quality of the Stokes radiation beam. As for the generation of the second Stokes component, experimental data pertaining to the mode of pumping by broadband chirped pulses are practically nonexistent. This mode has several differences from the case of pumping by narrow-band nanosecond and picosecond laser pulses. The aim of our work was to investigate the schemes and special features of the generation of the second Stokes component under broadband chirped pumping.

2. Experimental data and their discussion

Our experiments were carried out with the use of a Regulus RAPOP + Ti:sapphire laser system (Avesta-Project Ltd.). The system comprised a master oscillator, a system for pulse chirping (stretcher), a regenerative amplifier and a multipass one. The pulse energy at the output of the multipass amplifier exceeded 7 mJ for a pulse-repetition rate $f = 20 \text{ Hz}$. With the employment of only the regenerative amplifier, the maximum pulse energy amounted to 150 μJ for $f = 2 \text{ kHz}$. The chirped pulse duration at the

A.V. Konyashchenko P.N. Lebedev Physics Institute, Russian Academy of Sciences, Leninsky prosp. 53, 119991 Moscow, Russia; Avesta-Project Ltd., LPI premises, 142190 Troitsk, Moscow region, Russia; e-mail: fs@avesta.ru;

L.L. Losev P.N. Lebedev Physics Institute, Russian Academy of Sciences, Leninsky prosp. 53, 119991 Moscow, Russia; e-mail: losev@pluton.lpi.troitsk.ru;

S.Yu. Tenyakov 'Avesta-Project' Ltd., LPI premises, 142190 Troitsk, Moscow region, Russia; e-mail: tenyakov@avesta.ru

Received 18 February 2011

Kvantovaya Elektronika 41 (5) 459–464 (2011)

Translated by E.N. Ragozin

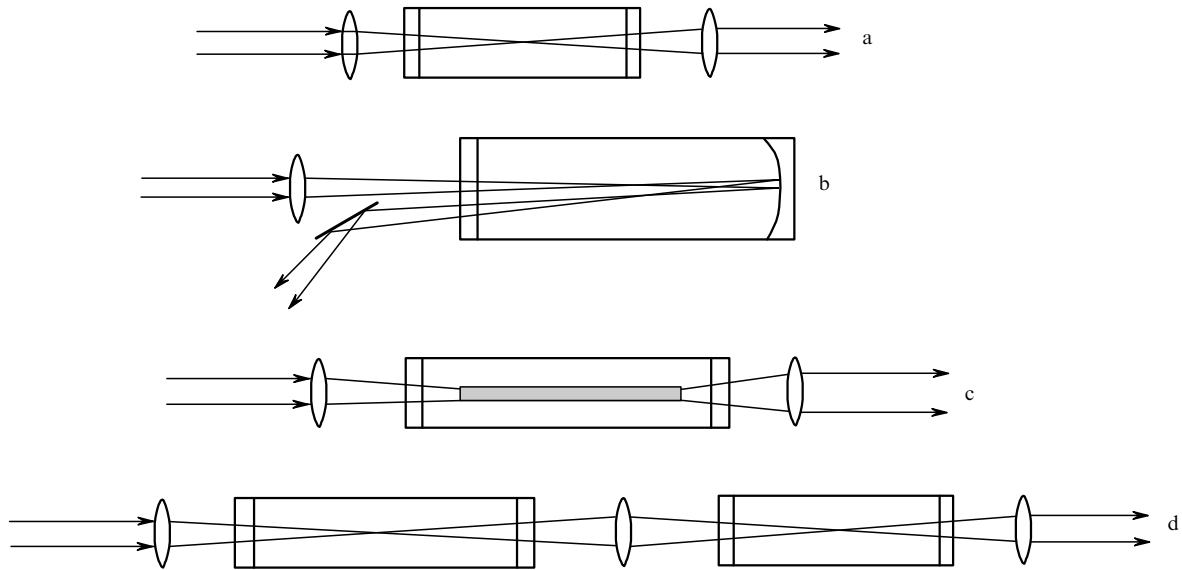


Figure 1. Optical schemes for the conversion to the second Stokes component: with one-fold focusing (a), two-fold focusing (b), a quartz capillary (c), and two cells (d).

output of the system was equal to ~ 100 ps, the spectral radiation width was ~ 300 cm^{-1} . The divergence of the light beam, which had a nearly Gaussian intensity distribution, was less than 1.5 times the diffraction limit.

Figure 1 shows the optical schemes of the sources of the second Stokes component investigated in our work. The Stokes radiation was generated for a single pass of the pump radiation through the active medium in all of the schemes [with one-fold focusing (Fig. 1a), two-fold focusing (Fig. 2b), a dielectric capillary (Fig. 1c), and two cells (Fig. 1d)]. The employment of external-cavity Raman converters was unfeasible because of the short pump pulse duration and frequency chirping. Given below are the results of investigation of each of the optical schemes depicted in Fig. 1.

2.1 Scheme with one-fold focusing

The generation scheme of Raman components with one-fold focusing of the pump radiation into the centre of the cell filled with an active medium has been most frequently employed and best studied. In this scheme, the second Stokes component was shown to initially develop due to a four-wave parametric process [10]. The experimental data given in Fig. 2 are consistent with this generation mechanism. We measured the pressure dependence of the efficiency of conversion to the first ($\lambda = 1.2$ μm) and second (2.5 μm) Stokes components in the focusing of chirped pump pulses with a 1.1-m focal-length lens to the centre of a 1.2-m long cell filled with pressurised hydrogen. The beam diameter was equal to 3 mm (at a $1/e^2$ intensity level), the pump pulse energy was equal to 5 mJ, and the pulse-repetition rate was 20 Hz.

As is evident from Fig. 2, the first and second Stokes components emerge at practically the same hydrogen pressure. This bears out the four-wave parametric mechanism of second Stokes component generation: under the parametric generation mechanism, the threshold pump energies (or the threshold value of the pressure of the active medium in the transient regime, which is realised in our

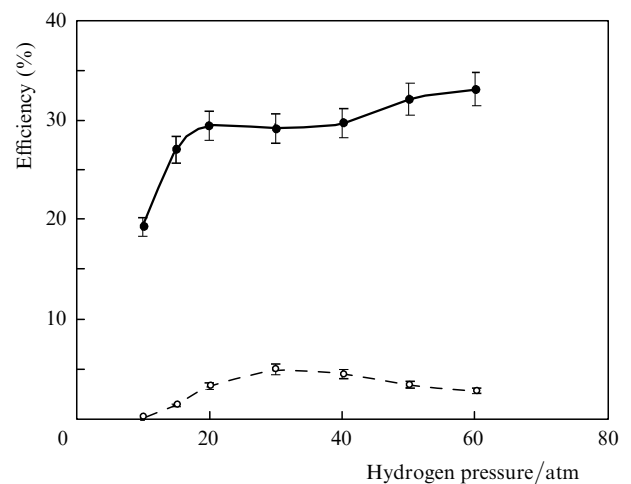


Figure 2. Efficiency of conversion to the first ($\lambda = 1.2$ μm , solid curve) and second (2.5 μm , dashed curve) Stokes components as functions of hydrogen pressure in the scheme with one-fold focusing for a pump pulse energy of 5 mJ and a pulse-repetition rate of 20 Hz.

case) should be close for the first and second Stokes components [11].

The highest energy efficiencies of conversion to the first and second Stokes components were equal to 32 % and 5 %, respectively. The advantages of this scheme of second Stokes component generation are the high conversion efficiency and its simplicity. A significant drawback consists in the quality of the light beam. It has been known [12] that the parametric generation regime, when there is a strong parametric coupling of the pump, Stokes, and anti-Stokes waves, is responsible for the annular structure of the spatial distribution of the beams of Raman components. In our case, measurements executed with the aid of an aperture of variable diameter showed that the distribution of the light beam both of the first and of the second Stokes components was a ring with a peak at the centre, the central peak accounting for no more than 20 % of the total energy. This

is the reason why the application of this scheme is seriously limited.

Similar dependences were obtained in the SRS of Ti:sapphire laser pulses in pressurised methane. The efficiency of conversion to the first Stokes component with a wavelength of 1.04 μm was equal to 38% and that to the second Stokes component with a wavelength of 1.5 μm was equal to 6%.

The transverse intensity distribution of the pump beam may be reproduced in the second Stokes component in the case of cascade generation mode. Assumed in this case is the absence of parametric coupling between the light beams and the sequential conversion of the pump pulse energy initially to the first and then to the second Stokes component. Cascade generation of the Raman components may be realised in a multipass cell. Under certain conditions, during the first passes of the pump through the active medium there occurs efficient generation of only the first Stokes component, which is converted to the second Stokes component during the subsequent passes [13]. In order to elucidate the feasibility of using a multipass cell for the Raman conversion of broadband chirped pulses, we investigated the SRS in a two-pass cell.

2.2 Scheme with two-fold focusing

The optical diagram of the experiment is schematised in Fig. 1b. The laser radiation was focused with a 60-cm focal-length lens into the centre of a 1-m long cell and was then incident on the surface of a mirror with a gold coating (with a radius of curvature of 50 cm) mounted at the end face of the cell. Upon refocusing by this mirror, the radiation was extracted from the cell at a small angle relative to the incident radiation.

The generation thresholds for the first and second Stokes components were measured for one- and two-fold focusing of the pump radiation. For an active medium, use was made of pressurised hydrogen. We found that the threshold energy of the pump pulse did not become lower as we passed from one-fold focusing to the two-fold one, i.e. the Stokes pulse generated in the first passage through the active medium did not interact with the pump pulse in the course of the second passage. The reason may be as follows. In the passage through the active medium of length L , between the pump pulse travelling with a group velocity v_p and the Stokes pulse with velocity v_s there occurs a delay $\Delta t = L(v_s^{-1} - v_p^{-1})$. For chirped pulses it results in a variation $\Delta\Omega = \Delta t d\omega/dt$, of the instantaneous frequency difference for these pulses, where $d\omega/dt$ is the chirp of the pump pulse and the Stokes component. When the frequency difference variation exceeds the width Γ of spontaneous Raman scattering, the Raman interaction between the pulses terminates. Hence there follows a limitation on the length of the active medium:

$$L < \Gamma \left[\frac{d\omega}{dt} \left(\frac{1}{v_s} - \frac{1}{v_p} \right) \right]^{-1}.$$

For gaseous hydrogen at a pressure of 60 atm, $\Gamma \approx 10^{-1} \text{ cm}^{-1}$ [14]. For $d\omega/dt = 3 \times 10^{12} \text{ cm}^{-1} \text{ s}^{-1}$ (spectrum width of 300 cm^{-1} , chirped pulse duration of 100 ps), the maximum length such that the Raman-interacting waves of the pump and the first Stokes component ($\lambda = 0.8$ and 1.2 μm , respectively) remain at resonance is equal to ~ 12 cm. In our scheme with two-fold focusing, on transit

through the gas layer between the two focal regions, which amounts to ~ 1 m in thickness, the Stokes wave generated in the first focal region will consequently not interact with the pump in the second focal region owing to its shift out of Raman resonance.

Therefore, the use of multipass cells is hardly promising for generating higher Raman components under broadband chirped pumping.

2.3 Scheme with a capillary

Cascade generation of the second Stokes component may also be realised in a scheme with a dielectric capillary. With the use of a capillary, the length of the region with a high pump intensity is longer in comparison with the one-fold focusing scheme. This permits attaining the gain increment required for the development of the second Stokes component from the level of spontaneous scattering. The lowering of SRS efficiency associated with the dispersion of the active medium manifests itself much weaker in the capillary than in multipass cells. This is due to the shorter capillary length, the absence of regions with a low radiation intensity, where the Stokes signal is not amplified (in the region of rapid growth of the Stokes wave there emerges the effect of nonlinear phase pulling [15]), and anomalous capillary dispersion, which partly compensates the normal dispersion of the active medium [16]. Furthermore, an advantage of the in-capillary conversion is the high quality of the light beam at the output, because the capillary acts like a spatial filter.

Figure 3 shows the experimental dependences of the efficiency of Ti:sapphire laser 800-nm radiation conversion to the first ($\lambda = 1.2 \mu\text{m}$) and second (2.5 μm) Stokes components on the pressure of hydrogen. The conversion was investigated using 25-cm long quartz capillaries with an inner diameter of 470 μm (Fig. 3a) as well as using 30-cm long capillaries of diameter 300 μm (Fig. 3b). The pump pulse energy was equal to 4 mJ for a pulse-repetition rate of 20 Hz. The capillary transmittance for the Ti:sapphire laser radiation was measured at 82% for the 300- μm diameter capillary and at 90% for the 470- μm diameter capillary.

The measured efficiency of conversion in capillaries is lower than that obtained for one-fold focusing, which is due to the losses in Stokes waves in their propagation through the quartz capillaries. The attenuation coefficient α is defined by the expression $\alpha \sim \lambda^2/a^3$ [17], where a is the capillary radius. This dependence may account for a more than two times lower efficiency of conversion to the second Stokes component in the 300- μm diameter capillary in comparison with the capillary of larger diameter. Despite the lower conversion efficiency, the scheme with a capillary may be employed owing to the high spatial quality of the light beams of the Raman components. In particular, our measurements showed that the light beam distribution at the output of the 300- μm diameter capillary is close to the Gaussian one.

Also among the virtues of the capillary scheme is the feasibility of converting low-energy laser pulses and raising the pulse-repetition rate. Lowering the energy of a pump pulse becomes possible due to the greater length of the high-intensity region in comparison with the length of the focal region in the focusing into free space. The pump-pulse-repetition rate in Raman converters involving gaseous media is limited by energy liberation in the region of generation of the Stokes radiation. This process is respon-

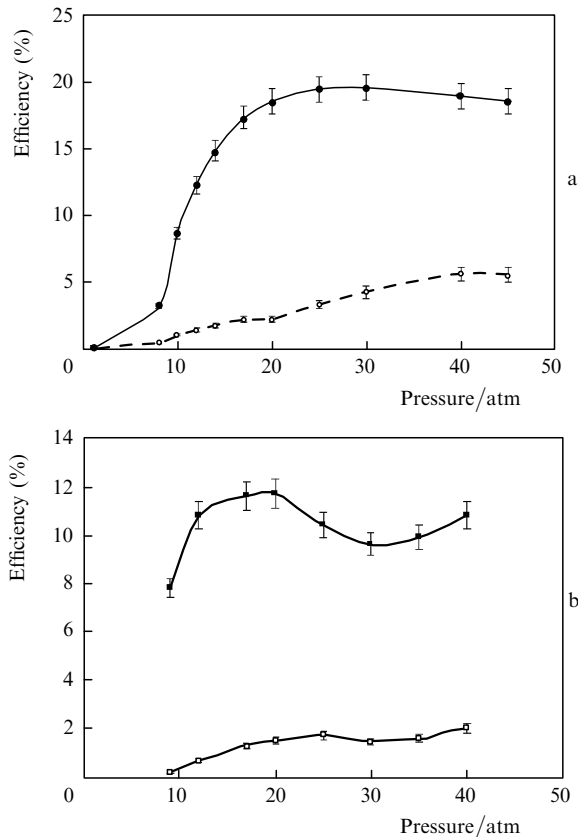


Figure 3. Efficiencies of conversion to the first ($\lambda = 1.2 \mu\text{m}$, solid curve) and second ($2.5 \mu\text{m}$, dashed curve) Stokes components as functions of hydrogen pressure in schemes with 470- μm diameter 25-cm long (a) and 300- μm diameter 30-cm long (b) quartz capillaries for a pump pulse energy of 4 mJ and a pulse-repetition rate of 20 Hz.

sible for nonuniform gas heating, optical nonuniformity, distortion of the optical beam, and the consequential lowering of the conversion efficiency. Our measurements showed that an appreciable lowering of the conversion efficiency in the scheme with one-fold focusing for a pump pulse energy of ~ 1 mJ becomes observable even beginning from a pulse-repetition rate of ~ 100 Hz. In capillaries there emerge no transverse convective flows and light beam distortions because of the uniform heating of the gas medium limited by capillary walls.

The conversion efficiency and the output beam intensity distribution in the converter investigated in our work, which employed a 10-cm long capillary 100 μm in diameter, remained invariable up to a pulse-repetition rate of 2 kHz – the maximum possible rate for the given Ti:sapphire laser. The energy of a single pump pulse was independent of the pulse-repetition rate and was equal to 150 μJ . Figure 4 shows the pressure dependences of the average output Stokes radiation power for this converter for a pulse-repetition rate of 2 kHz. In this case, the efficiency of conversion to the second Stokes component was equal to 2.5%. As noted above, the moderate efficiency was due to the growth of losses in the capillary with increasing wavelength. Nevertheless, the converter compactness (cell length of 20 cm, external diameter of 2 cm), the relatively high average power and the high beam quality make this IR radiation source quite suitable for certain applied problems.

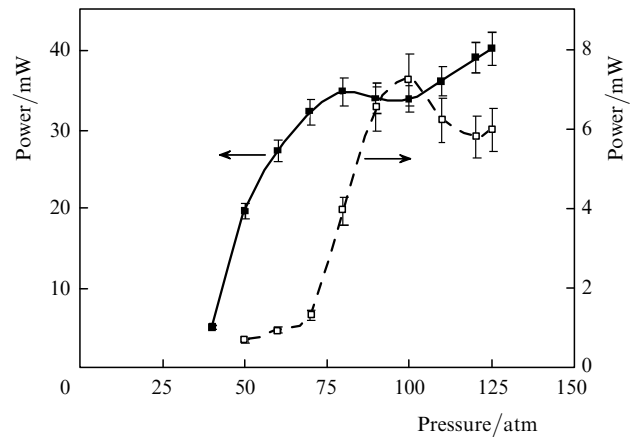


Figure 4. Average power of the first ($\lambda = 1.2 \mu\text{m}$, solid curve) and second ($2.5 \mu\text{m}$, dashed curve) Stokes components as functions of hydrogen pressure in the SRS in a 10-cm long capillary of diameter 100 μm . The average pump power is 300 mW, the pulse-repetition rate is 2 kHz. KEY

2.4 Scheme with two cells

The use of gas Raman-active media opens the possibility of making sources of the second Stokes component comprising two sequentially arranged optical cells. By independently varying the pressure, the composition of the gas medium, and the cell length it is possible to maximise the efficiency of generation of only one Stokes component in each of the cells and thereby optimise the cascade generation of the second Stokes component.

Cascade generation of the second Stokes component was experimentally investigated according to the scheme depicted in Fig. 1d with the use of a 1.2-m long cell (the first stage of conversion) and a 0.3-m long cell (the second stage). The pump was provided by a MATEKO-10 (Avesta-Project Ltd.) Ti:sapphire laser, which generated 100-ps long chirped pulses with an energy of 7 mJ at a pulse-repetition rate of 15 Hz. The central wavelength was equal to 0.79 μm and the spectrum width was 300 cm^{-1} . The light beam was Gaussian, 3 mm in diameter.

The 1.2-m long first cell effected conversion to the first Stokes component with a wavelength of 1.18 μm . The pump radiation was focused at the cell centre with a 1.5-m focal length lens. As is well known [18], to achieve a high efficiency of conversion of a Gaussian light beam to the first Stokes component reproducing the wavefront of the pump, the pump pulse energy should exceed the threshold energy by 2–3 times and the parametric coupling of the Stokes and anti-Stokes components should be eliminated. For a fixed energy of the pump pulse, the requisite excess over the SRS-threshold energy is achieved by selecting the pressure of the working gas, and Raman-parametric processes are suppressed by adding a buffer gas possessing a high dispersion. Krypton was selected as the buffer gas. Under our experimental conditions, the optimal SRS regime was achieved for a hydrogen pressure of 10 atm on addition of krypton at a pressure of 10 atm. For these figures, the energy efficiency of converting the pump to the first Stokes component was equal to 34%. The divergence of the Stokes light beam with a close-to-Gaussian intensity distribution did not exceed 1.5 diffraction limits.

The radiation of the first Stokes component was focused into the second cell with a 50-cm focal length lens. Figure 5 shows the pressure dependences of the efficiency of con-

version to the second Stokes component with a wavelength of 2.3 μm . In this case, the buffer gas was not needed owing to the high working pressure of hydrogen. The second Stokes component was generated under two pumping regimes. Under the first regime, focused into the cell was the radiation of only the first Stokes component emanating from the first cell (single-frequency pumping). The Ti:sapphire laser radiation unconverted in the first cell was rejected with a colour glass filter. Under the second regime, there was no spectral filtration of radiation (two-frequency pumping). The highest conversion efficiency under the single-frequency regime was equal to 25 %, which was one and a half times higher than the highest conversion efficiency under the two-frequency pumping equal to 17 %. The lower conversion efficiency under the two-frequency pumping may be due to the reverse conversion of the first Stokes component to the initial laser radiation. This conversion proceeds on the dynamic polarisability lattice, which is written in the active medium of the second cell in the SRS of the unconverted pulse of the laser radiation outgoing from the first cell. And this pulse precedes the pulse of the first Stokes component. The phase matching condition is automatically fulfilled for this four-wave process. The lowering of the oscillation threshold for the second Stokes component under the two-frequency pumping also counts in favour of this explanation. (In this case, the second Stokes component emerges at a lower hydrogen pressure.) The lowering of the SRS threshold in converters with biharmonic pumping takes place in the case of low-intensity radiation, which is usually longer in wavelength than the strong pump [19].

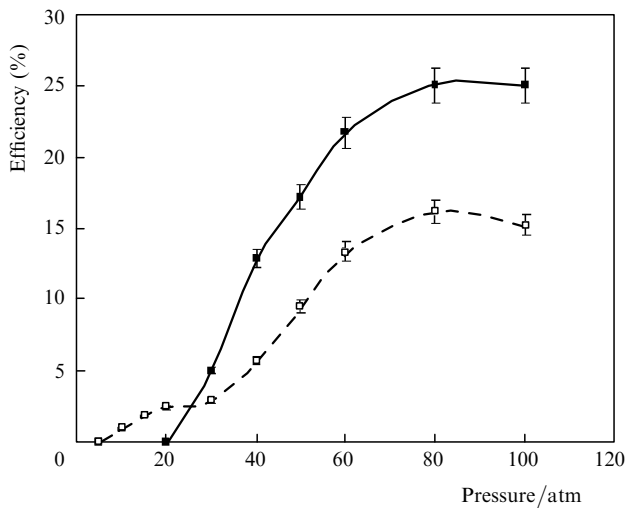


Figure 5. Pressure dependences of the efficiency of conversion to the 2.3- μm Stokes radiation in the second cell in the scheme with two cells under single-frequency (the first Stokes component with $\lambda = 1.18 \mu\text{m}$, solid curve) and two-frequency (the first Stokes component and the initial laser radiation with $\lambda = 0.79 \mu\text{m}$, dashed curve) pumping.

The measured quantum SRS conversion efficiency (the ratio between the number of Stokes photons and the number of pump photons) in each of the cells was equal to $\sim 50\%$ both for the 0.79-to-1.18 μm radiation conversion and for the 1.18-to-2.3 μm radiation conversion. As a result, the quantum efficiency of conversion to the second Stokes component of the whole system amounted to 25 % and the

energy efficiency to 8.5 %. In this case, the light beam of the second Stokes component had a bell-shaped spatial distribution without rings surrounding the central part.

The use of the optical scheme with two cells also makes it possible to employ combinations of two different gases. In particular, we converted the Ti:sapphire laser radiation to the 1.8- μm wavelength radiation in the cascade SRS in compressed methane (at the first stage) and hydrogen with an energy efficiency of 12 %.

3. Conclusions

We have investigated optical schemes intended for the generation of the second Stokes component under pumping by broadband chirped pulses. The energy conversion efficiency and parameters of the light beam were measured for one- and two-fold pump radiation focusing into the active medium as well as in the scheme with a quartz capillary and the scheme with two optical cells. The highest conversion efficiency was attained in the scheme with two cells. The chirped pulsed Ti:sapphire laser radiation with a central wavelength of 0.79 μm was converted to the second Stokes component with a wavelength of 2.3 μm with an efficiency of 8.5 % in the SRS in pressurised hydrogen. Employing the scheme with a capillary enabled raising the pulse-repetition rate up to 2 kHz with retention of the diffraction-limited beam quality of the second Stokes component.

We also mention that preliminary experiments in the generation of the second Stokes component in methane under two-pulse pumping [7] yielded chirped pulses of the second Stokes component with a spectrum width equal to the spectrum width of the pump pulse – the pulse of Ti:sapphire laser with a spectrum width of 300 cm^{-1} . It is anticipated that the pulse of the second Stokes component will be shortened to 50–70 fs upon temporal pulse compression. This will open the door to the SRS-based generation of high-power femtosecond light pulses in the 1.5–3- μm wavelength range.

Acknowledgements. The authors express their appreciation to M.N. Gerke for placing at our disposal a femtosecond laser facility for the execution of our experiments.

References

1. Popmintchev T., Chen M.-C., Cohen O., Grishan M. E., Rocca J.J., Murnane M.M., Kapteyn H.C. *Opt. Lett.*, **33**, 2128 (2008).
2. Chen M.-C., Arpin P., Popmintchev T., Gerrity M., Zhang B., Seaberg M., Popmintchev D., Murnane M.M., Kapteyn H.C. *Phys. Rev. Lett.*, **105**, 173901 (2010).
3. Yakovlev V.S., Ivanov M., Krausz F. *Opt. Express*, **15**, 15351 (2007).
4. Sugiharto A.B., Johnson C.M., De Aguiar H.B., Alloatti L., Roke S. *Appl. Phys. B*, **91**, 315 (2008).
5. Imahoko T., Takasaso K., Sumiyoshi T., Sekita H., Takahashi K., Obara M. *Appl. Phys. B*, **87**, 629 (2007).
6. Jordan C., Stankov K.A., Marowsky G., Canto-Said E. *J. Appl. Phys. B*, **59**, 471 (1994).
7. Konyashchenko A.V., Losev L.L., Tenyakov S.Yu. *Opt. Express*, **15**, 11855 (2007).
8. Konyashchenko A.V., Losev L.L., Pazyuk V.S., Tenyakov S.Yu. *Appl. Phys. B*, **93**, 455 (2008).
9. Konyashchenko A.V., Losev L.L., Tenyakov S.Yu. *Kvantovaya Elektron.*, **40**, 700 (2010) [*Quantum Electron.*, **40**, 700 (2010)].

10. Andreev R.B., Gorbunov V.A., Gulidov S.S., Papernyi S.B., Serebryakov V.A. *Kvantovaya Elektron.*, **9**, 56 (1982) [*Sov. J. Quantum Electron.*, **12**, 35 (1982)].
11. Guntermann C., Schulz-von der Gathen V., Dobele H. F. *Appl. Opt.*, **28**, 135 (1989).
12. Chiao R.Y., Stoicheff B.P. *Phys. Rev. Lett.*, **12**, 290 (1964).
13. Antognini A. et al. *Opt. Commun.*, **253**, 362 (2005).
14. Murray J.R., Goldhar J., Eimerl D., Szoke A. *IEEE J. Quantum Electron.*, **15**, 342 (1979).
15. Butylkin V.S., Venkin G.V., Kulyuk L.L., Maleev D.I., Khronopulo Yu.G., Shalyaev M.F. *Kvantovaya Elektron.*, **4**, 1537 (1977) [*Sov. J. Quantum Electron.*, **7**, 867 (1977)].
16. Burzo A.M., Chugreev A.V., Sokolov A.V. *Opt. Commun.*, **264**, 454 (2006).
17. Marcatili E.A.J., Schmeltzer R.A. *Bell Syst. Tech. J.*, **43**, 1783 (1964).
18. Zel'dovich B.Ya., Pilipetskii N.F., Shkunov V.V. *Obrashchenie volnovogo fronta* (Wave Front Reversal) (Moscow: Nauka, 1985).
19. Venkin G.V., Krochik G.M., Kulyuk L.L., Maleev D.I., Khronopulo Yu.G. *Pis'ma Zh. Eksp. Teor. Fiz.*, **21**, 235 (1975).